31.5 GHz-50.0 GHz Ortho-Mode Transducer for the Nanocosmos receiver in the 40m Radiotelescope

S.Lopez-Ruiz, F.Tercero, M.G. Nuñez, J.A. Lopez-Fdez

IT- CDT 2017-1

Observatorio de Yebes
Apdo. 148 19080 Guadalajara
SPAIN
Phone: +34 949290311 ext. 203545
email: samuel.lopez@oan.es

Turnstile-based waveguide orthomode transducer (OMT) is described for the WR22 standard rectangular waveguide. The OMT is designed as part of the Q-band receiver for the 40m radiotelescope. The designed orthomode transducer exhibits a return loss better than 20 dB at any port, an insertion loss less than 0.7 dB, and an isolation of 25 dB over the full bandwidth.

January 12, 2017

Contents

List of Figures

List of Tables

Chapter 1

Introduction

This technical report shows the design, construction and measurement of a Q-band Orthomode covering the whole band of the rectangular waveguide WR-22, exceeding 1.5 GHz in the lower part of the band (31.5-50 GHz).

1.1 Motivation

The need for this work arises from the collaboration of the Yebes Observatory with Nanocosmos project which pretends to simulate the conditions of vacuum, temperature and ultraviolet radiation occurring in the interstellar medium within a special laboratory chamber, in order to know the Physical-chemical processes that give rise to the dust grains and to the compounds or molecular species existing in said medium. These laboratory observations will be complemented with astronomical observations with the radio telescope of 40 meters where it is expected to identify new molecular species observed both in the laboratory chamber as in astronomical observation [1, 2]. These observations are ambitious from the point of view of the bandwidth that we want to process simultaneously in each observation, so that the passive components of the new receivers to be used in Nanocosmos must fulfill their specifications in whole waveguide used in the design. In this case, WR-22 waveguide, with the above mentioned additional use of 1.5 GHz in the lower part of the band.

1.2 Background

Currently, the Q-band receiver operating on the 40m radio telescope since 2015 is the result of an upgrade to adapt it to the M4 branch of the radio telescope during the project carried out together with the Korean Astronomical and Space Institute (KASI). As a part of the KVN baseline extension project (Korean VLBI Network) and its use for multifrequency phase reference technique. Current installed Q-band receiver [3, 4] is a moderate bandwidth receiver covering 41.00-49.00 GHz. It is circular polarization receiver and it is devoted to astronomical and VLBI use. Its specifications are described in the

Table 1.1. The passive components used (phase-corrected corrugated horn and circular septum polarizer) currently limit the receiver utilization band to its nominal band.

Table 1.1: Q band receiver Specifications

Frequency Band	Q band: 41-49 GHz
Physical Temperature	<65 K radiation shield <22 K cold stage
Pressure	$<10^{-6} mbar$
LNA Gain (COLD+ROOM)	29.5 + 24.3 dB LCP 27.5 + 22.8 dB RCP
Noise Temperature	RCP: <60 K LCP: <60 K
Inputs	Q band: Feed RCP calibration: 2.4mm LCP calibration: 2.4mm
Outputs	RCP : 2.4mm LCP : 2.4mm
Impedance	50Ω

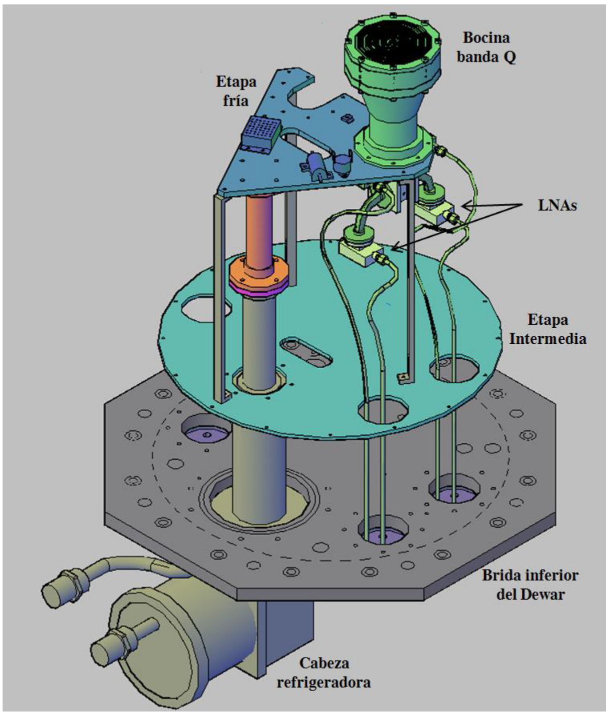

Figure 1.1: Q band Receiver

Septum polarizer is a three-port device, one port is used to feed the horn waveguide (circular or square) and the other two ports (semicircular or rectangular) receive signals that correspond to the LHCP or RHCP components of the input waveguide (Figure 1.2). The sheet that divides the cavities (septum) is usually very thin (compared to the wavelength). So it complicates its construction in high frequencies, being preferable other designs. Bandwidth depends on the return losses, cross-talk between channels and desired axial ratio specifications. The usually handled value is 20%, it is difficult to increase it even by increasing the complexity of the septum sheet [5].

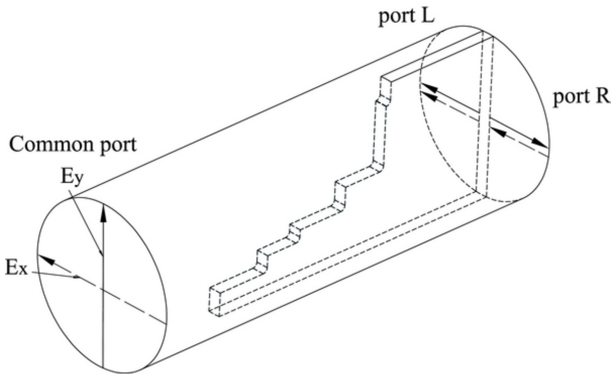

Figure 1.2: Septum Polarizer

As an alternative to the septum polarizer, we chose to have linear polarization in receiver and obtain it through an OMT (Ortho Mode Transducer). These devices achieve bands close to 45% in the designed waveguide. To achieve circular polarization at these receivers, a phase shifter will be inserted to obtain the signals proportional to the RHCP and LHCP polarization input at the OMT outputs. This separation layout is necessary for present VLBI observations and it is limited in band by the operation of the phase shifter. The following figure describes its operation (Figure 1.3).

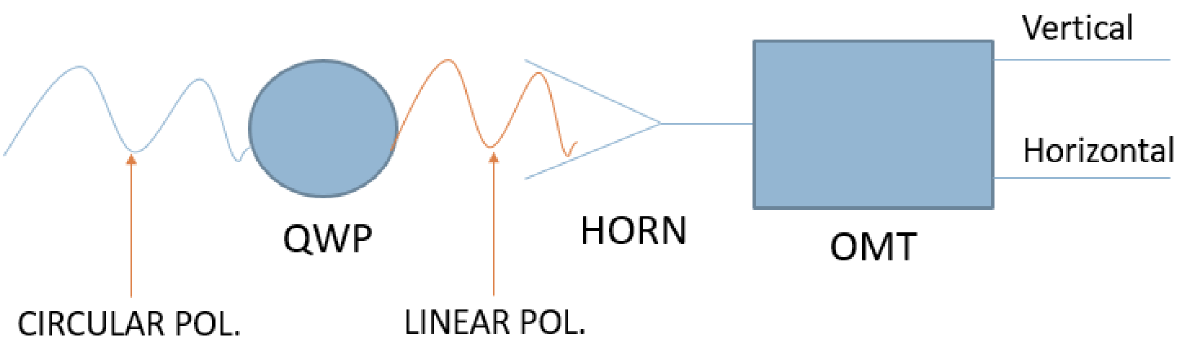

Figure 1.3: Polarizer (QWP+OMT)

1.3 OMT Types

There are different types of waveguide devices to achieve the separation of both linear polarizations. It presents a non-exhaustive review of the alternatives that have been valued for the construction: T-junction or side-coupling, Boifot and Turnstile.

The simplest OMT configuration is a T-Junction or side-coupling OMT (Figure 1.4). The incident TE_{10} fundamental mode at common port having the polarization along y-direction propagates in the common waveguide and couples to the fundamental mode TE_{10} of the rectangular waveguide port 3. The TE_{10} mode in the common waveguide does not couple to the fundamental mode TE_{10} of the rectangular waveguide port 4.

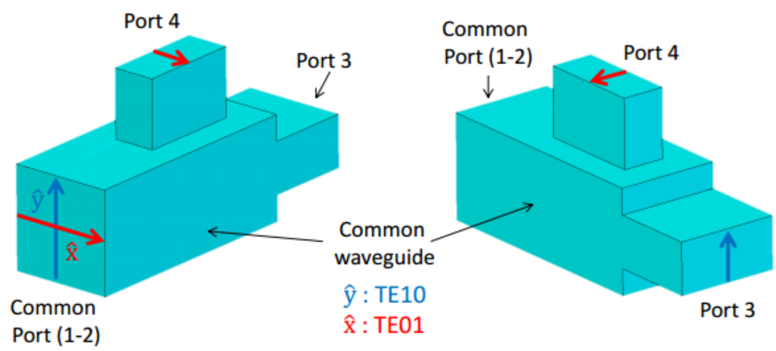

Figure 1.4: Standard T-junction OMT

On the other-hand, the incident TE_{10} mode at common port having the polarization along x-direction couples to the side arm's fundamental mode TE_{10} of the rectangular waveguide port 4 and this polarization is under cut-off at port 3. Hence, port 3 and 4 are also isolated only if the fundamental mode is under consideration.

Although side-coupling OMTs are quite simple and compact, they only work in narrow frequency bands. Their operative bandwidth can be increased by introducing some matching element like septa, irises and steps. In this way, the operative bandwidth can be enlarged up to 20% (Figure 1.5). In any case, because of the one-fold symmetrical structure (other-fold assymetrical), the bandwidth is limited due to the cutoff frequency of the higher-order modes TM_{11} and TE_{11}.

Boifot junction based OMT is exploited to enlarge the operative band. Symmetric E-plane coupling is used for the polarization along the x-direction shown in (Figure 1.6). This kind of coupling provides two fold symmetry that avoids the excitation of the TE_{11} and TM_{11} higher-order modes in the common port. Therefore in this configuration the bandwidth can be enlarged up to the TE_{20} cutoff frequency. On the other hand, the two symmetric side arms need to be recombined, by exploiting the straight and bent rectangular waveguide sections in order to obtain a single signal at port 4. Therefore this structure is more complex.

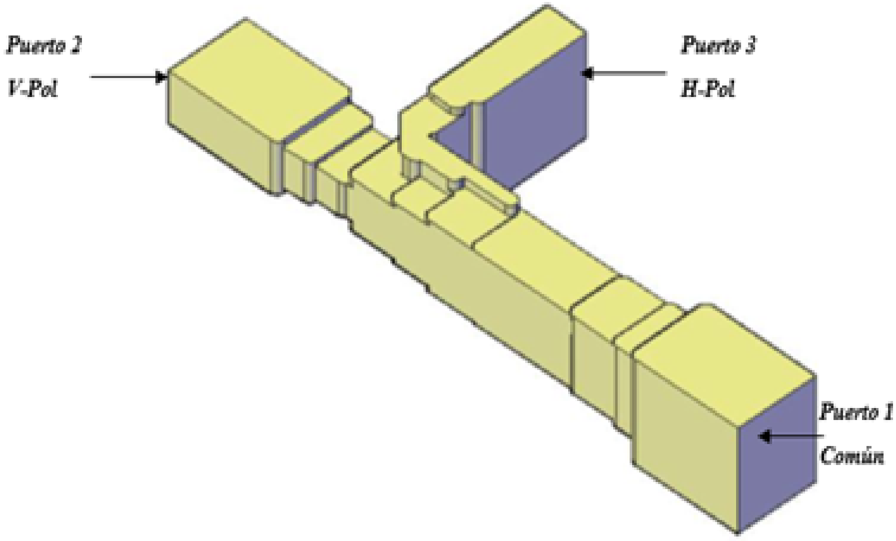

Figure 1.5: T-junction OMT with steps

It should be noticed that any differential error in the length of the two waveguides of the combining network due to the machining inaccuracy could destroy the symmetry of the structure and, consequently, a performance degradation would be observed. Additionally, insertion loss and group delay are intrinsically quite different for both polarizations.

In Turnstile Based OMT configuration, a turnstile junction is used to separate the two orthogonal polarized signals into two separate waveguides. It has a common square/circular waveguide port and four rectangular waveguide ports as reported in Figure 1.7.

Physical ports are five, whereas six electrical ports are necessary if only fundamental mode TE_{11} is considered. The turnstile junction exploits a symmetric E-plane coupling for both polarizations. For a perfectly symmetric structure, the incoming x-polarized signal couples to the fundamental TE_{10} mode at port 1 and port 2 as reported with dotted line in Figure 1.7. Same polarization excites the TE_{01} mode at ports 3 and 4 but this mode is under cut-off in the operative frequency range of the structure. Hence, the power is equally split between port 1 and port 2, but the signals at port 1 and at port 2 are in counter-phase. Similarly, the incoming y-polarized signal couples to the fundamental TE_{10} mode at the ports 3 and 4. In particular, half signal flows to port 3 and the other half is routed to port 4, but the two coupled signals are in counter-phase.

Since the turnstile junction has two-fold symmetry, it inherently has a very good isolation level. The TE_{11} mode in circular waveguide does not excite the TM_{01} and TE_{21} modes in the common waveguide. Therefore, the upper limit of the frequency band is related to the cutoff frequency of the TM_{11} mode at the common port and the cutoff frequency of the TE_{10} mode at the coupled ports.

Two different waveguide structures (not shown in Figure 1.7) are required to combine the opposite ports. Also in this case, possible asymmetries of the combiners owing to

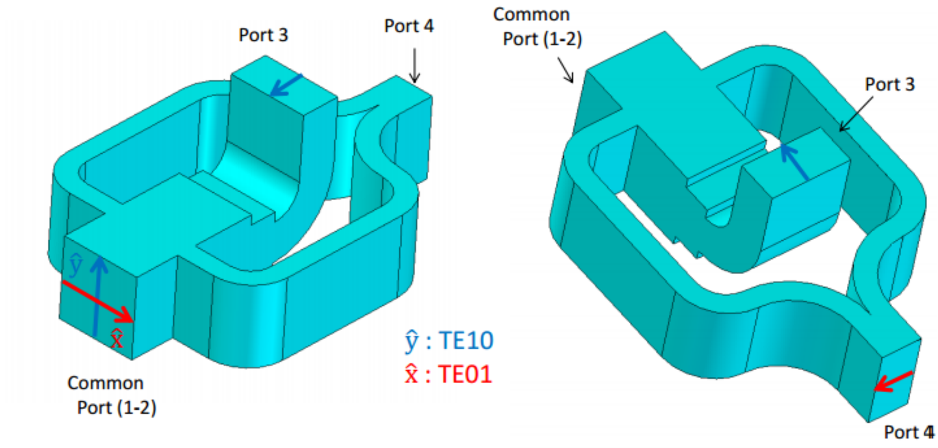

Figure 1.6: Structure of the Boifot OMT

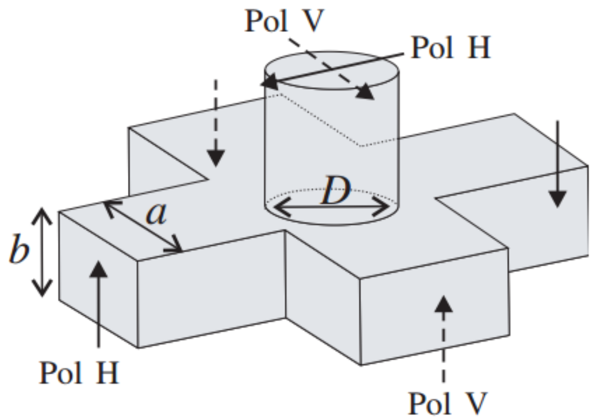

Figure 1.7: Turnstile Junction

the manufacturing uncertainties should be managed to avoid isolation problems. This OMT type can operate in a large frequency band with good power handling properties. However, the presence of two combiners makes this configuration less compact and with higher losses.

Usually a proper protrusion with either pyramidal, cylindrical or parallelepiped shapes can be introduced in the back of the junction in order to improve the matching. Turnstile junction exhibits the same insertion loss and group delay for both polarizations since the latter undergo a symmetric coupling at the same section of the common port. Various shape and combination of shapes of matching elements are reported in literature (pyramidal [6], cylindrical [7], multisection cylindrical [8], square prism [9]).

Based on Table 1.2, that summarizes the main characteristics of the revised OMTs, the device selected after this review was the Turnstile Based OMT because it is the only one with the ability to reach 45% of bandwidth.

Table 1.2: Performance Q Band OMT

Types / Performance	Side-Coupling OMT	Boifot OMT	Turnstile Based OMT
Return Loss	>15 dB	>20 dB	>20 dB
Insertion Loss	<0.35 dB	<0.99 dB	<0.2 dB
Isolation	>32 dB	>50 dB	>40 dB
Fractional Bandwidth	<0.2	0.4	>0.4
Critical Element	No	Septum	Pin

1.4 OMT Turnstile

There are different techniques but the one that achieves the most bandwidth is place an obstacle in the input waveguide. There are designs with a square prism, [9], pyramids and cylinders as compensation elements [7] as indicated in the previous section.

Once the signal is divided between the four arms, the signals that were divided between facing arms in phase opposition must be combined. There are several proposals in the literature.

In [9], signals from opposing ports reach the combiner via a continuous E-plane bend. Combiner has a taper in rectangular sections to hold the height of the standard waveguide. All rectangular waveguide sections have the standard height (Figure 1.8). Results obtained are reflections greater than 19 dB, losses less than 0.15 dB and isolation greater than 48 dB in a bandwidth of 38%.

In [10], E-plane bends are implemented with optimized chamfers. In addition, reduced height waveguides are used to simplify the design of the combiner. They get results in a bandwidth of 45% (Figure 1.9).

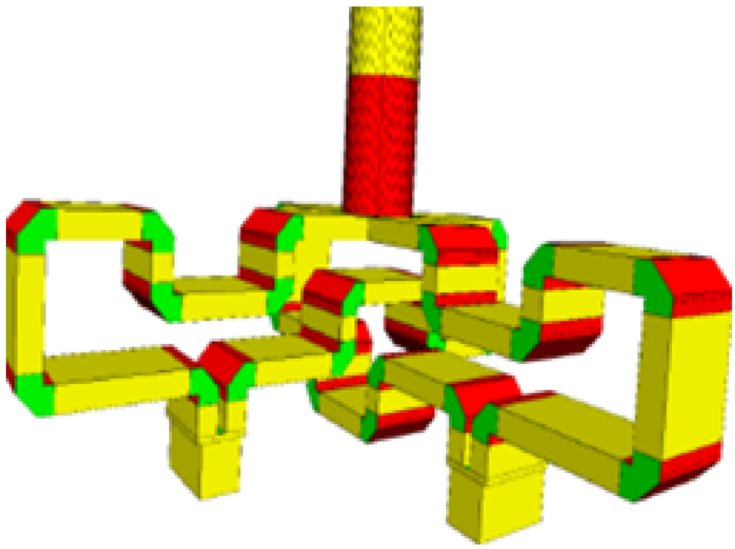

Figure 1.9: Turnstile Junction Waveguide Orthomode Transducer

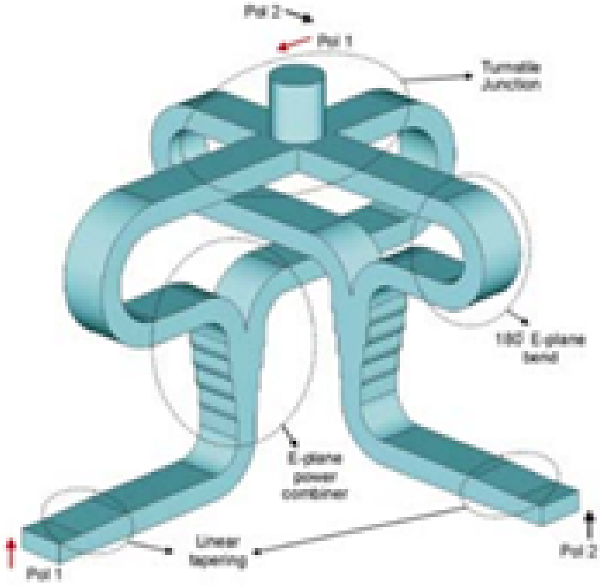

Figure 1.8: Turnstile Junction Waveguide Orthomode Transducer

In [11], ways of reaching the combiner are shown using curved waveguides in the H-plane, also with reduced height waveguides to the combiner. In this case the obtained bandwidth is smaller (Figure 1.10).

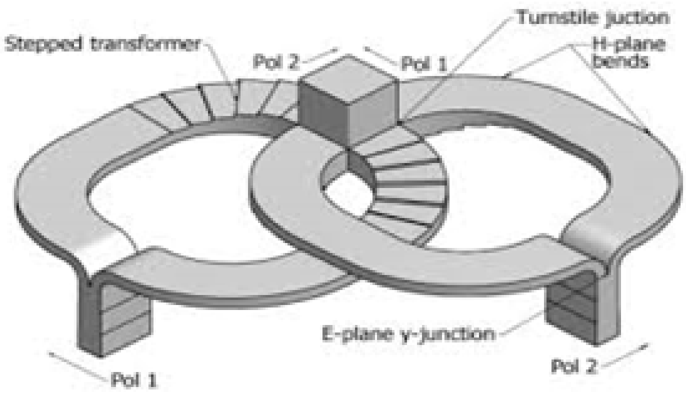

Figure 1.10: Turnstile Junction Waveguide Orthomode Transducer

For all these considerations, the design is based on the design criteria of [10].

1.5 Specifications

Geometric specifications will be set by the dimensions of rectangular waveguides (WR-22) and circular waveguide of Q-band horn. In the case of electrical specifications, they are set by the standard goals for passive components in radio-frequency receivers with special care with the minimization of losses. The standard nomeclature for multi-mode ports will be used for the S parameters according with the Figure 1.11 where in each physical port there may be more than one electric port depending on the considered modes.

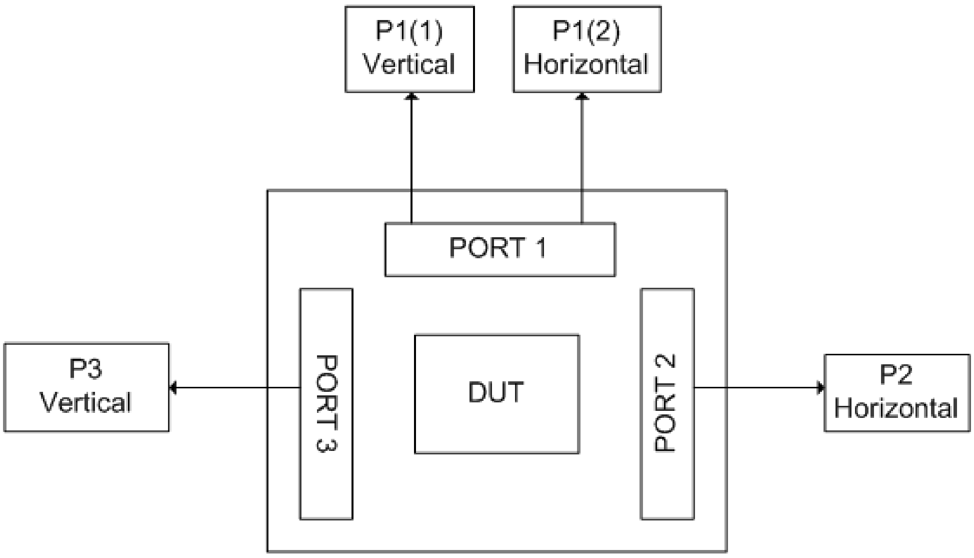

Figure 1.11: S-Parameters Definition

For example, input and output port 1, and the input mode 1 and the output mode 2 correspond to the parameter: **S1(1)1(2)**.

Table 1.3: Specifications

Number	Definition	Parameter	Value
1	Waveguide Output Dimensions	a x b	5.69x2.84 mm (WR-22)
2	Waveguide Input radius	dcirc	6 mm
3	Input reflection losses	S1(1)1(1) and S1(2)1(2)	$<$ -20 dB
4	Output reflection losses	S22 and S33	$<$ -20 dB
5	Insertion losses	S1(1)3 and S1(2)2	$<$ -0.5 dB
6	Isolation	S1(2)3 and S1(1)2	$<$ -30 dB
7	Frequency Range	$f_{up} - f_{down}$	50-31.5 GHz

Chapter 2

Design

Most parts of the OMT design was carried out using CST Microwave Studio (CST MWS). CST MWS is based on the Finite-Difference Time-Domain Method (FDTD) [12]. CST MWS is well suited for electrically large structures and features a powerful, parametric drawing editor to lay out the structures.

The design of the complete OMT was done in several steps. First, the modes that are propagated are analyzed, then the components that form the OMT (union turnstile, bend and combiner) will be designed and optimized. With all the elements simulated independently will be joined to form a circuit model. Finally, the 3D model is constructed to obtain a refined solution. Note that the numbering of the ports in the design of the elements does not correspond to the final numbering that the ports of the device have. During design, appropriate port designations are chosen to facilitate understanding during the design phase.

2.1 Waveguide Modes

Figure 2.1 shows the main modes for a circular waveguide and a rectangular waveguide at the design frequency.

According to specifications the diameter of the circular waveguide is 6mm to be able to be attached directly to the horn and the rectangular guide will be 5.69x2.84 mm. In Table 2.1 and Table 2.2 the cutoff frequencies of the modes that are excited in rectangular and circular waveguides respectively are indicated.

Table 2.1: Cutoff Frequencies for rectangular waveguide

Modes	f/f_c	**Frequency (GHz)**
TE_{10}	1	26.28
TE_{01} & TE_{20}	2	52.56

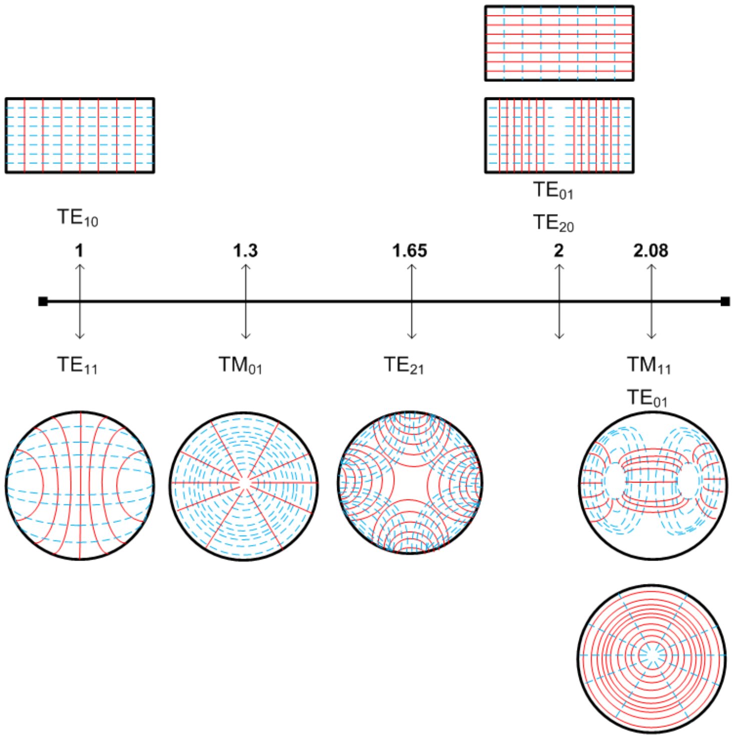

Figure 2.1: Cutoff frequencies for the first higher-order modes of the waveguide

Table 2.2: Cutoff Frequencies for circular waveguide

Modes	f/f_c	**Frequency (GHz)**
TE_{11}	1	29.26
TM_{01}	1.3	38
TE_{21}	1.65	48.279
TM_{11} & TM_{01}	2.08	60.8

In rectangular waveguide the next mode that propagates is twice the frequency, this corresponds to frequencies greater than 50 GHz therefore it is not necessary to analyze them.

In circular waveguide the next mode that is propagated is to 38 GHz and 48.279 GHz. In theory, these modes can be excited due to the discontinuity created in the unions. However, its excitation can be avoided as long as the symmetry of the structure is strictly maintained. In fact, the isolation and adaptation bandwidth is essentially determined by the possible excitation of higher order modes. The four metallic cylindrical sections located at the base of the circular wave guide do not break this symmetry as long as we ensure good electrical contact between the circular sections and the turnstile junction.

A more conservative design criterion is to maintain the cutting frequency of TE21 mode above the upper frequency. In our case because the OMT and feed have to operate up to 31.5 GHz we keep the output waveguide at a slightly higher diameter.

2.2 Elements

The design of the OMT structure was divided into three main blocks: turnstile, E-plane bend, and Y-junction power combiner (Figure 2.2). All these blocks were designed and optimized individually using CST MWS. Once these blocks are designed, the full OMT is implemented, simulated, and refined using the same software.

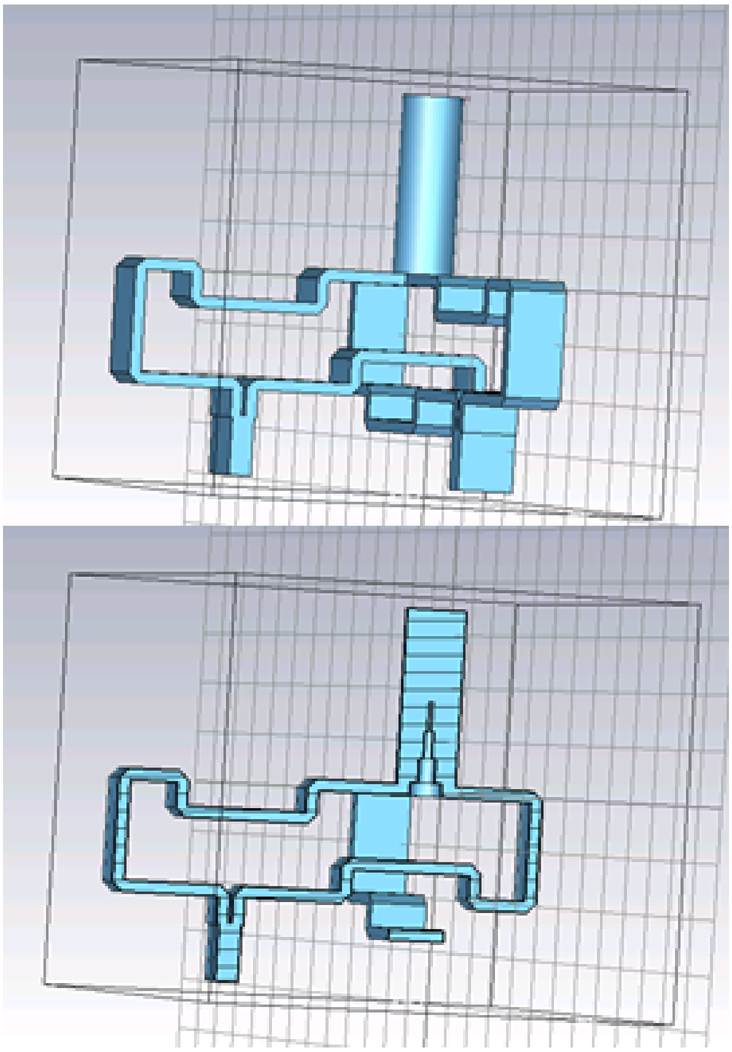

Figure 2.2: Final OMT model simulated in CST

OMT configuration has three physical waveguide ports (Figure 2.3). OMT is therefore used to route the two orthogonally polarized field components at the common port to two different waveguide ports. The routing of the various signals is obtained introducing suitable apertures and discontinuities between the common waveguide and the coupled waveguides.

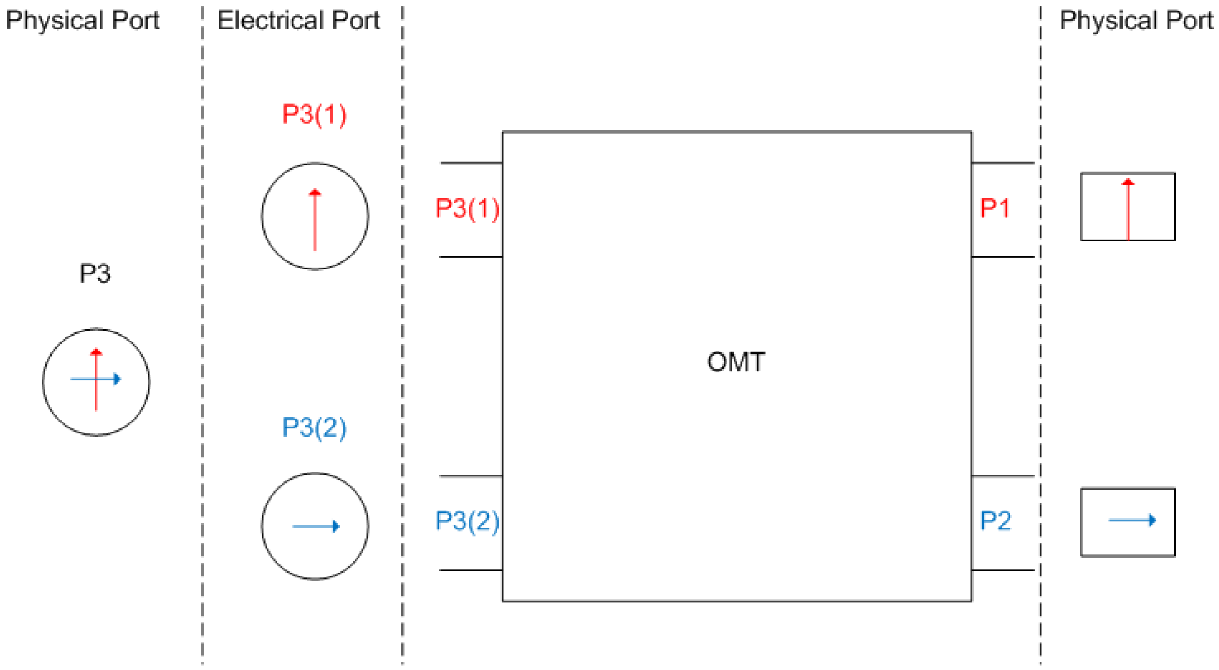

Figure 2.3: OMT Ports Scheme. The common port (P3) has two electrical ports P3 (1) and P3 (2) corresponding to the two vertical polarizations (Red) and horizontal (Blue). There are two output ports, one for vertical polarization (P1) and one for horizontal (P2).

2.2.1 Turnstile Junction

Turnstile junction divides the input signal into its orthogonal polarizations (Figure 2.4). This element has bad reflection characteristics so an obstacle is introduced that increases the band. In [13] the different obstacles and their behavior in the face of the loss of reflection are studied. It has been verified how the cylindrical obstacles allow a greater band and that with four concentric cylinders are enough for the design band. A greater number of cylinders would imply a mechanical limit since the section would be very small and hardly mechanizable.

Additionally, obstacle acts as a tuning stub enabling selection of the working bandwidth without changing the orthomode transducer structure. Therefore, the bandwidth can be shifted or modified by simply changing the scatterer. Mode TE_{11} at common port (Port 5 of Turnstile Junction) will be separated into two orthogonal signals, 5(1) and 5(2), having the same cutoff frequency. 5(1) is split equally and in antiphase between both branches of the arms. The same argument applies to 5(2).

Turnstile junction shown in Figure 2.5 has been simulated. The S-Parameters (dB) results and the parameters that define the Junction are in **Appendice A**.

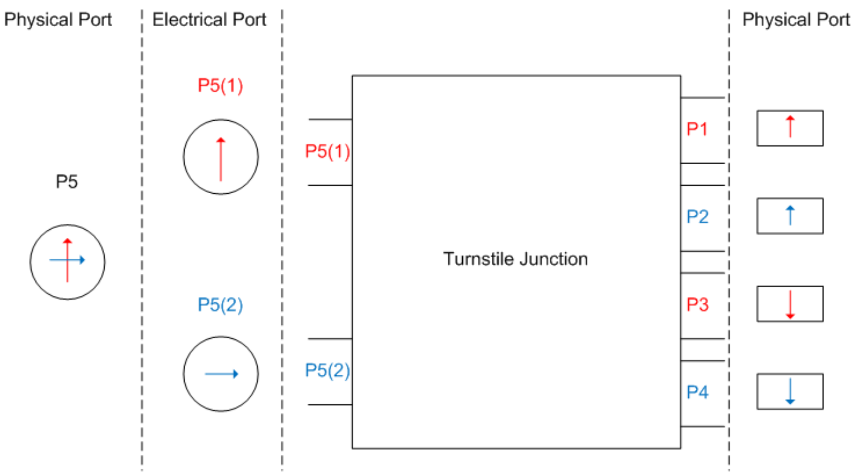

Figure 2.4: Turnstile Junction Ports Schema. Common port (P5) has two electrical ports P5 (1) and P5 (2) corresponding to the two vertical polarizations (Red) and horizontal (Blue). There are 4 output ports, two for vertical polarization (P1/P3), where the electrical component of P3 is 180° out of phase with P1 and two for horizontal (P2/P4) with identical behavior.

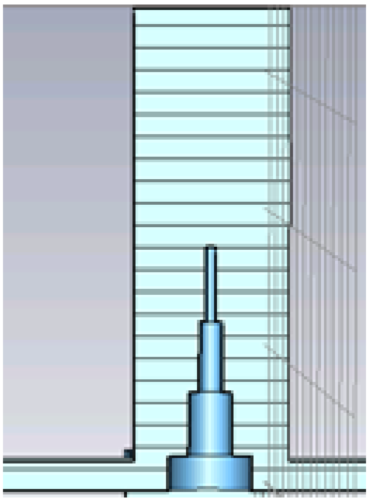

Figure 2.5: OMT Turnstile Junction Model

Results obtained are indicated in Table 2.3.

2.2.2 E-Bend Arm

The presented OMT is completely designed using E-plane bends and reduced height waveguides. The main advantage of this strategy is to increase the usable bandwidth, in **Appendice B** the difference between E-plane bends and a H-plane bends is analyzed [14].

Table 2.3: OMT Turnstile Junction Results

Parameter	Definition	Value (dB)
S5(1)5(1)	Return Loss	>20
S5(2)5(2)		>20
S11 & S33		>5
S22 & S44		>5
S5(1)1 & S5(1)3	Insertion Loss	$\simeq -3$
S5(2)2 & S5(2)4		$\simeq -3$
S5(2)1 & S5(2)3	Isolation	>60
S5(1)2 & S5(1)4		>60

All bends in the designed OMT are identical and follow the structure of Figure 2.6.

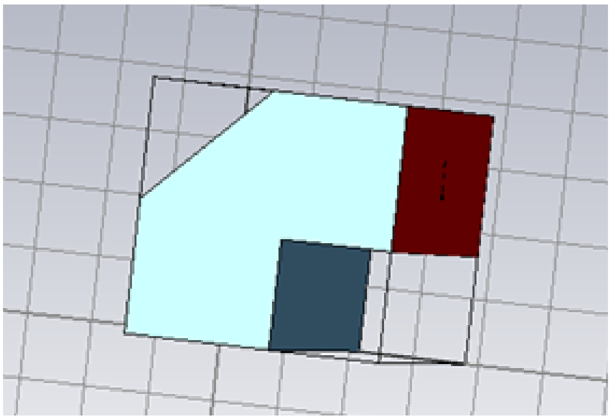

Figure 2.6: E-Bend arm

In [15] an analysis of different geometries of bends is made, finally this one was chosen by its simplicity in the machining. This structure has been optimized for broadband performance, results and parameters are in **Appendice B**.

The results obtained are indicated in Table 2.4:

Table 2.4: E-Bend Results

Parameter	Definition	Value (dB)
S11 & S22	Return Loss	>40
S12 & S21	Insertion Loss	<0.05

2.2.3 Combiner

Power combination is carried out by using single stepped E-plane Y-junctions. Another advantage of the use of reduced height waveguides is that they give good results with very compact structures. This combiner needs only one step matching compared with more complex designs. Ports 2 & 3 correspond to half-waveguides and Port 1 to WR-22 waveguide. Figure 2.7 shows the model of the designed Y-junction. Simulation results of the power combiner are in **Appendice C**.

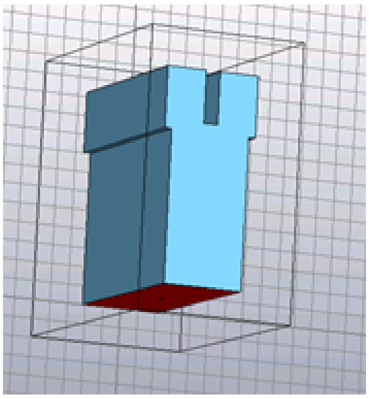

Figure 2.7: Combiner

Summary of Results (Table 2.5):

Table 2.5: Combiner Results

Parameter	Definition	Value (dB)
S11	Return Loss	>50
S22 & S33		$\simeq -6$
S13 & S12	Insertion Loss	$\simeq -3$

2.3 Simulation

Once the elements were optimized separately, they were joined in the schematic of the Figure 2.8.

There are 4 branches. Branches 1 and 3 correspond to vertical polarization and 2 and 4 to horizontal. The branch 1 and 2 are equal in number of elements that compose it and the same thing happens with the branches 3 and 4. The 4 branches have the same length, this fact is very important so that the signal is summed in phase in the combiner .

In the schematic, it is necessary to incorporate a phase shifter to take into account that by one of the paths the signal is shift 180º.

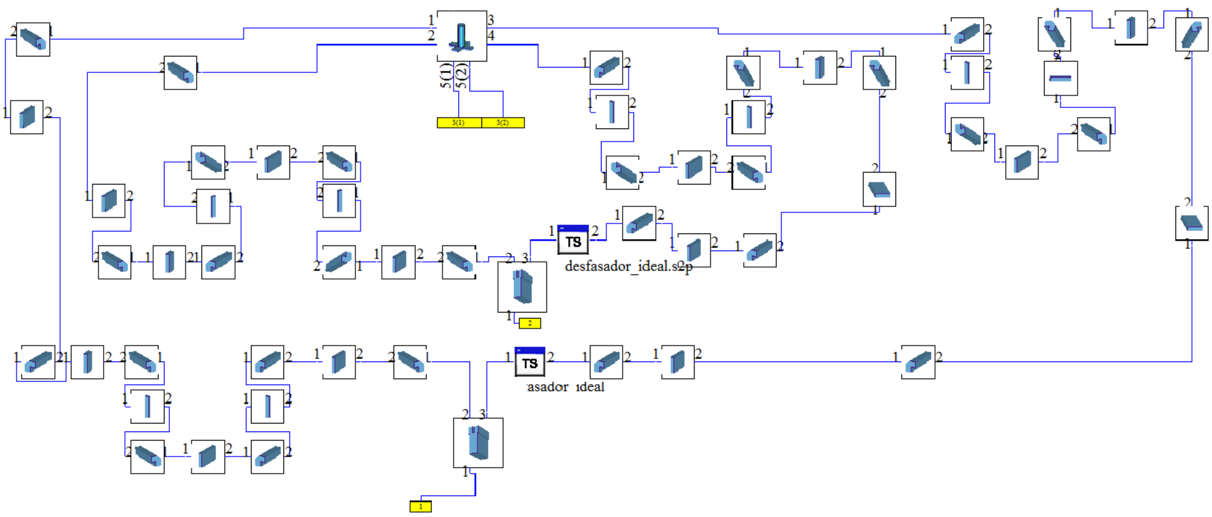

Figure 2.8: Schematic

Finally, the total model was optimized to improve the behavior of the entire OMT, return losses, insertion losses and isolation were minimized. The results obtained are in Table 2.6.

Table 2.6: OMT Results

Parameter	Definition	Value (dB)
S3(1)3(1) & S3(2)3(2) S11 & S22	Return Loss	>20 >20
S3(1)1 & S3(2)2	Insertion Loss	<0.1
S3(2)1 & S3(1)2	Isolation	>40

In **Appendice D**, a schematic of all elements that compose the OMT, the final values of the parameters that define each element and S-parameters of final simulated OMT are shown.

Finally an analysis of sensitivity of the possible imperfections in the manufacture of the OMT has been done and they have been simulated to know the impact that they have, results are in Appendice **Appendice E**. For example as the isolation can increase by varying the length of one the waveguides, and also a misalignment of the central pin.

Chapter 3

Mechanical Design

OMT body is divided into four pieces which join along the circular waveguide axis and consequently split the rectangular waveguides at their E-field mid-plane. This gives minimum resistive losses in the waveguides and allows the use of standard mechanical machining techniques to be used. Each piece is physically different (Figure 3.1). Aluminum was chosen as the body material for its availability, excellent mechanical properties, and ease of surface treatment (Aluminium 6082-T6).

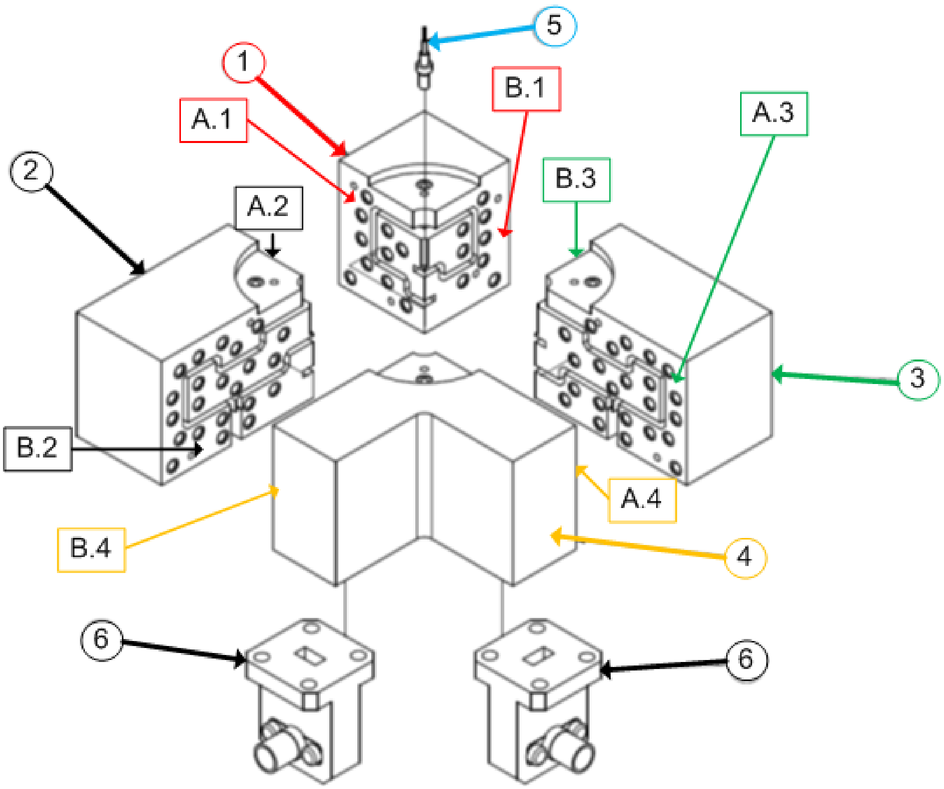

Figure 3.1: OMT pieces

In order to obtain a suitable adjustment and tolerance result the following manufacturing guide is written: Each part of the assembly shall be defined as indicated in Table 3.1.

Table 3.1: Pieces and Faces

Piece	Face
1	A.1 B.1
2	A.2 B.2
3	A.3 B.3
4	A.4 B.4
5	-

The dimensions and treatment of the surfaces must be made with the maximum possible precision. For this reason the following manufacturing sequence has been listed:

1- **Phase 1: Piece preparation.**

1.1- Preparation of the four pieces as blocks with three faces as reference planes and other three faces letting them grow around. The lengths will be sufficient to ensure the final nominal dimension and perpendicularity between faces (i.e. greater than 0.1mm per face).

2- Phase 2: A.1 Machining

2.1- The reference planes are palpated to determine the zero of the part, which does not correspond to surface A.1 or B.1.

2.2- A planned on face A.1 will be executed until the nominal block dimension is achieved with precision.

2.3- The milling of the guides of the face A.1 will be carried out, the surfaces of the guides must have a maximum surface finish. The holes that accommodate the adjustment pins will be made.

2.4- Then the holes that accommodate the screws of face A.1 will be realized. These screws are NOT threaded.

2.5- End of phase 2. Figure 3.2.

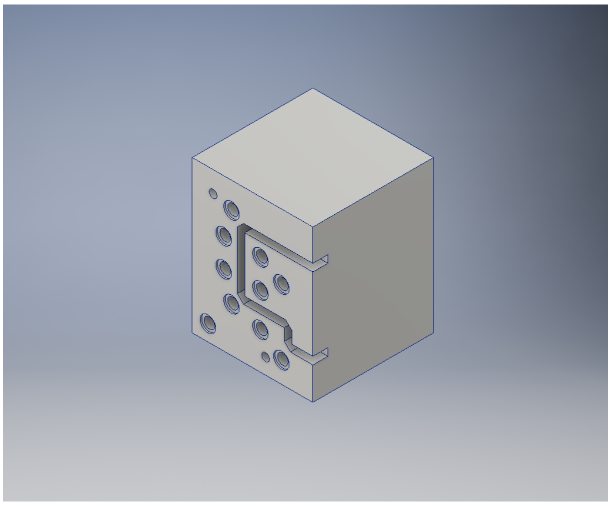

Figure 3.2: Phase 2 Piece

3- Phase 3: A.2 Machining.

3.1- The operations of the previous phase are replicated in face A.2.

3.2- The adjustment pins (ISO 2338 - 1.5 h8 x 10) will be inserted, and then the parts P1 and P2 will be joined. In case of a play between pieces, they will be adjusted by matching the outer reference planes.

3.3- Both pieces will be fixed using the M2 screws (DIN 912 - M2 x 8).

3.4- End of phase 3. Figure 3.3.

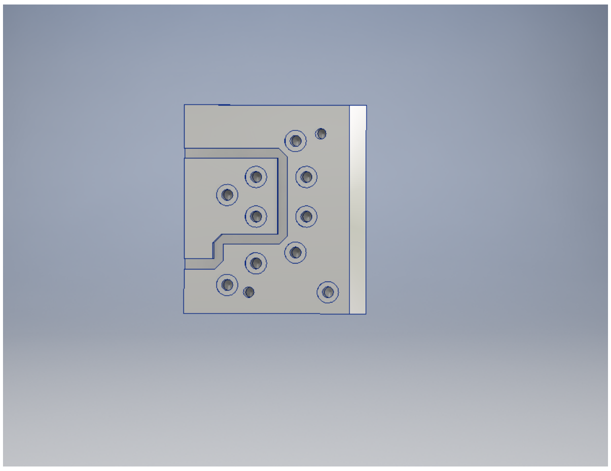

Figure 3.3: Phase 3 Piece

4- Phase 4: A.3 Machining.

4.1- The operations of phase 2 are replicated in face A.3.

4.2- End of phase 4. Figure 3.4.

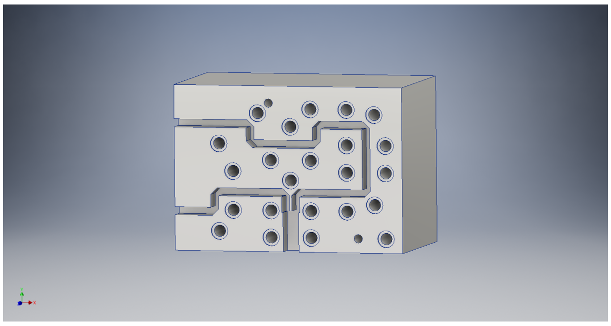

Figure 3.4: Phase 4 Piece

5- Phase 5: A.4 Machining.

5.1- The operations of phase 2 are replicated in face A.4.

5.2- The adjustment pins (ISO 2338 - 1.5 h8 x 10) will be inserted, and then the parts P3 and P4 will be joined. In case of a play between pieces, they will be adjusted by matching the outer reference planes.

5.3- Both pieces will be fixed using the M2 screws (DIN 912 - M2 x 8).

5.4- End of phase 5. Figure 3.5.

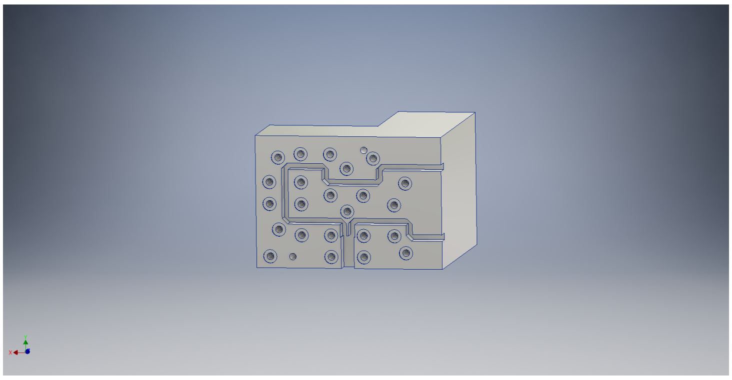

Figure 3.5: Phase 5 Piece

6- Phase 6: B.1 + B.2 Machining.

6.1- The reference planes are palpated to determine the zero of the part, which does not correspond to the surface B.1 or B.2.

6.2- A planned one on the face B.1-B.2 will be achieved until the nominal block dimension is achieved with precision.

6.3- The joint milling of the inner face guides formed by the pieces P1 and P2 will be carried out, all the surfaces thereof must have a maximum surface finish.

6.4- The holes that accommodate the adjustment pins of faces B.1 and B.2 will be made.

6.5- The holes on both sides are then drilled. They are NOT threaded.

6.6- The depth of the mechanized ducts shall be checked.

6.7- End of phase 6. Figure 3.6.

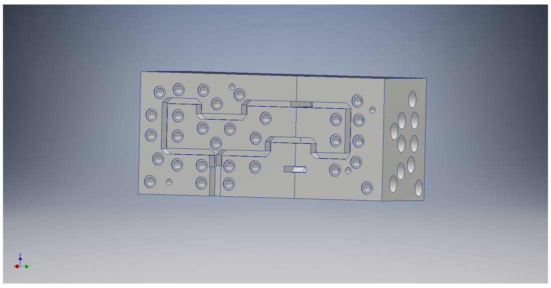

Figure 3.6: Phase 6 Piece

7- Phase 7: B.3 + B.4 Machining.

7.1- The reference planes are palpated to determine the zero of the part, which does not correspond to the surface B.3 or B.4.

7.2- A planned one on the face B.3-B.4 will be achieved until the nominal block dimension is achieved with precision.

7.3- The joint milling of the inner face guides formed by the pieces P1 and P2 will be carried out, all the surfaces thereof must have a maximum surface finish. The holes that accommodate the adjustment pins of faces B.3 and B.4 will be made.

7.4- The holes on both sides are then drilled. They are NOT threaded.

7.5- The depth of the mechanized ducts shall be checked. The adjustment pins (ISO 2338 - 1.5 h8 x 10) will be inserted, and then the sets P1-P2 + P3-P4 will be joined.

7.6- Both sets will be fixed using the screws M2 (DIN 912 - M2 x 8 & (DIN 912 - M2 x 12).

7.7- End of phase 7. Figure 3.7.

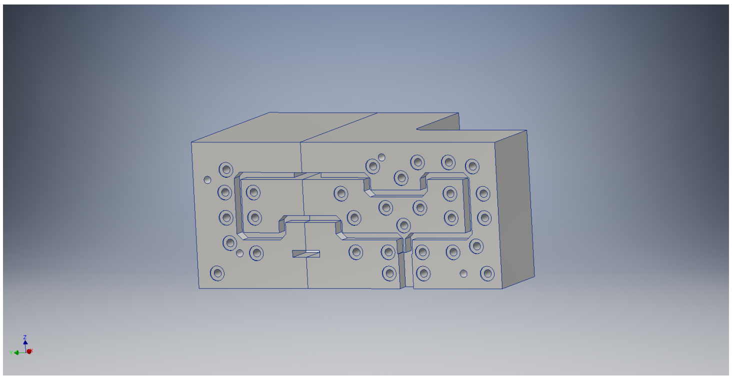

Figure 3.7: Phase 7 Piece

8- Phase 8: P1+P2+P3+P4 Top Machining.

8.1- The block is palpated to determine that it meets the nominal dimensions of its reference planes. Next determine the point of attachment of the four pieces for the beginning of the circular flange.

8.2- Milling of the upper circular cage of the assembly [P1 + P2 + P3 + P4] (depth 2mm).

8.3- The external threaded bores will be realized.

8.4- Circular groove milling (depth 4mm) of the assembly [P1 + P2 + P3 + P4] (depth 4mm).

8.5- The central threaded bore or reamer for the insertion of the obstacle, depending on the type of obstacle.

8.6- A planning is done to eliminate any possible burrs produced in the machining, giving the surface of the face a maximum surface finish that allows the greatest contact between faces.

8.7- The P5 part of the Ortomode shall be fixed and the fastening pins (ISO 2338 - 1.5 h8 x 10) of the upper face shall be fixed with a pinion, to protect the part P5.

8.8- End of phase 8. Figure 3.8.

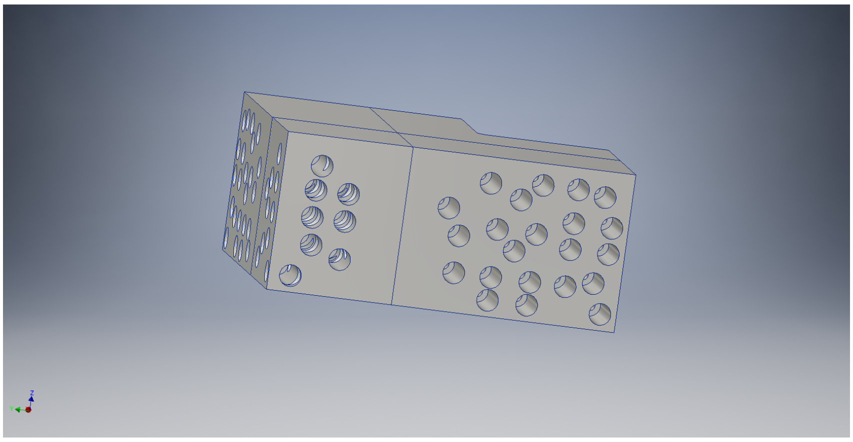

(a) ***Union of the pieces***

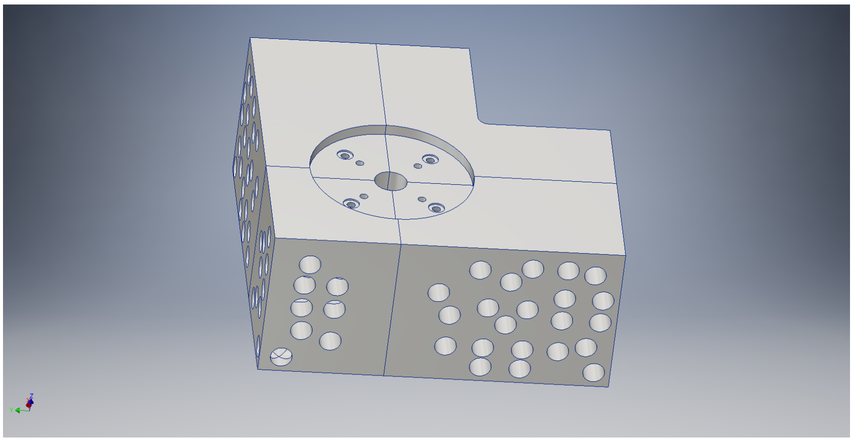

(b) ***Top Machining***

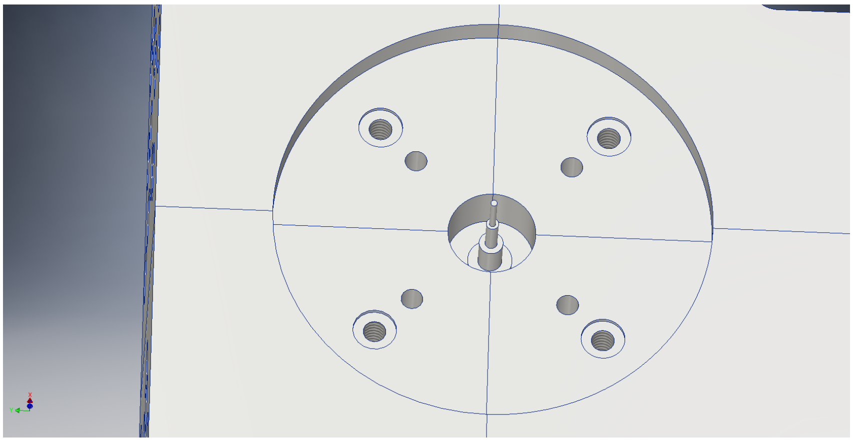

(c) ***Obstacle***

Figure 3.8: Phase 8 Piece

9- Phase 9: P1+P2+P3+P4 Below Machining.

9.1- Making the threaded bores in the set [P1 + P2 + P3 + P4]. In order to realize these threaded bores, the inside of the waveguide can be palpated or a mandrel can be used on the guide to mark the holes.

9.2- A planning is done to eliminate any possible burrs produced in the machining, giving the surface of the face a maximum surface finish that allows the greatest contact between faces.

9.3- End of phase 9. Figure 3.9.

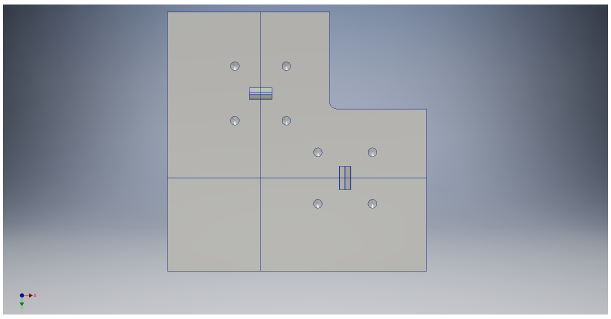

Figure 3.9: Phase 9 Piece

10- Phase 10: Transition Machining.

10.1- Realization of the transition to be able to fit it to a horn.

10.2- Couple transition to OMT.

10.3- End of phase 10 and end of machining. Figure ref fig: P10.

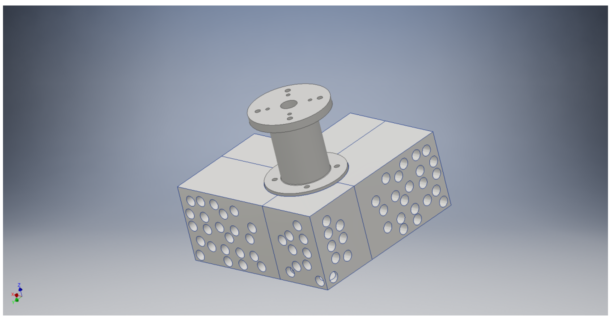

Figure 3.10: Phase 10 Piece

The final machining of the OMT is represented in Figure 3.11.

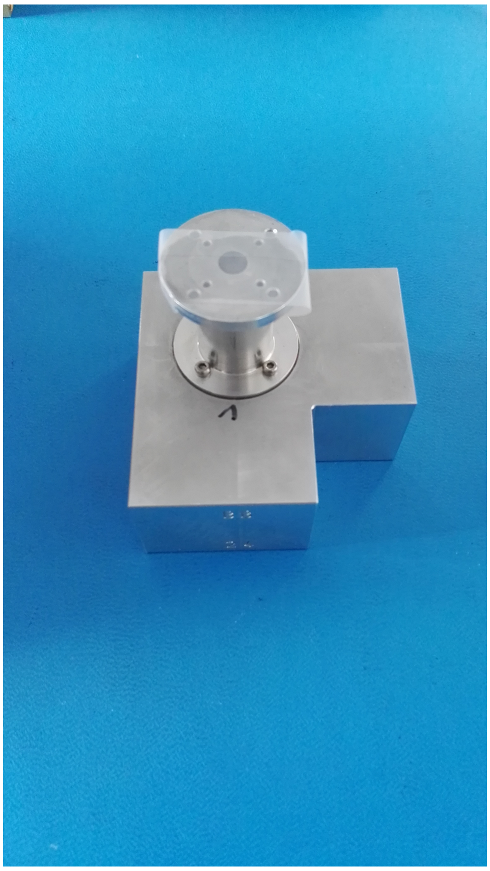

(a) ***Port 1***

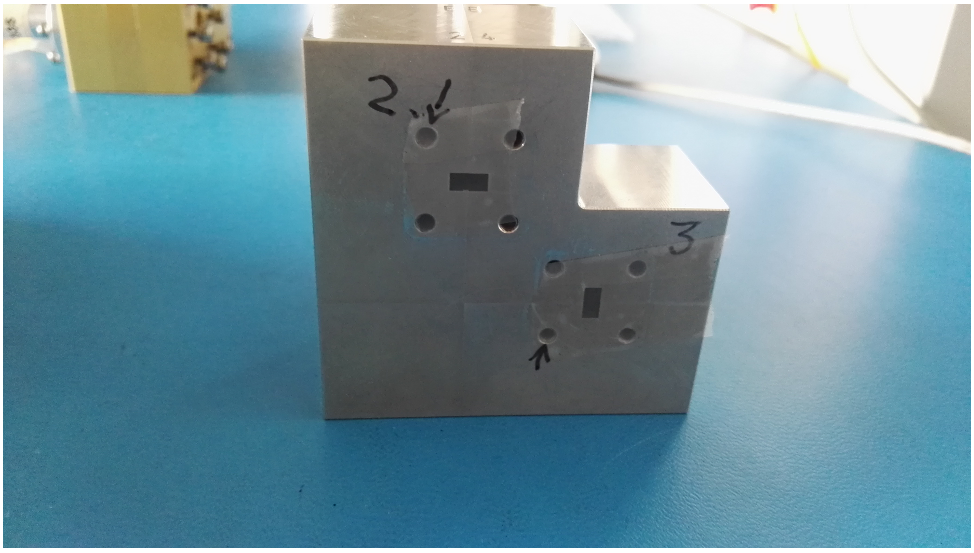

(b) ***Port 2 & 3***

Figure 3.11: OMT Mechanical

Chapter 4

Measurements

Two OMTs were manufactured (A and B item). It allows the possibility of almost full S-parameter characterization on all the OMTs by measuring the OMTs individually and in pairs (Back-to-Back).

All the measurements have been taken with a 2-port vector network analyzer (E8364B PNA from Agilent Technologies).

The components used for the measurement are:

1- OMT A and B.

2- TRL calibration kit. Specific calibration waveguide short and 1/4 wavelength waveguide **Appendice F.1**.

3- One circular-to-rectangular waveguide transition **Appendice F.2**.

4- Two rectangular waveguide load **Appendice F.2**.

5- One set of coax-to-waveguide adapters **Appendice F.3**.

6- Circular waveguide load **Appendice F.3**.

4.1 Measurementes Description

All measurements have been made for both orthogonal polarizations: Vertical (Port 3) and Horizontal (Port 2). In Figure Figure 1.11 and 3.11 you can find the numbering of the ports. There are 4 types of measurement. The first three correspond to the measure of the individual OMT and the fourth to the measure of the Back-to-Back.

4.1.1 Insertion Losses OMT individually

For this measure OMT must be connected to the PNA as indicated in Figure 4.1:

The circular port was connected to the analyzer through a circular-to-rectangular waveguide transition. The rectangular port of the OMT connected to the analyzer and

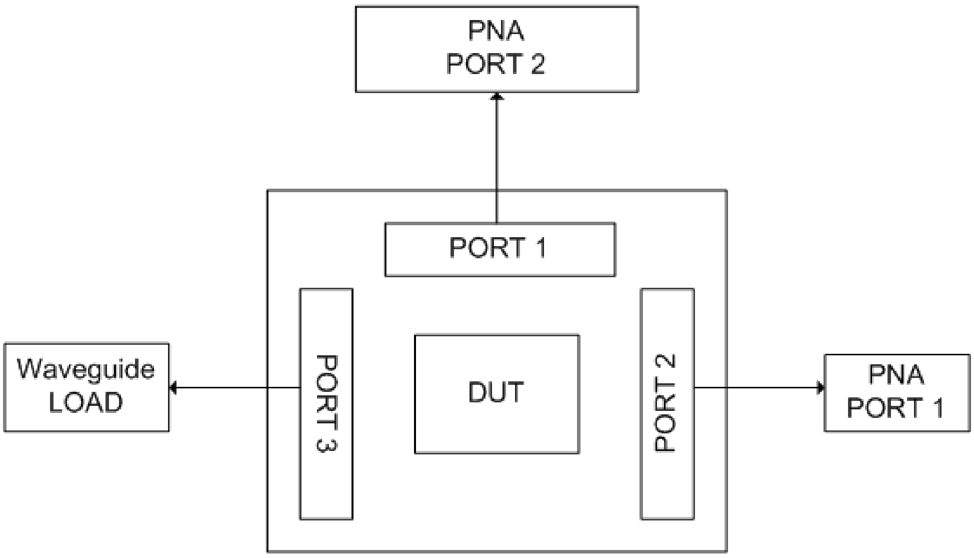

Figure 4.1: Schematic of Insertion Loss Measurements of the OMT Indiviudally

the rectangular waveguide of the transition circular-to-rectangular was connected to the coax-to-waveguide adapters. The rectangular port of the OMT not connected to the analyzer was terminated with a rectangular waveguide load.

For the measurement of the Horizontal Polarization (Port 2 of the OMT) the scheme of Figure 4.1 will be followed. To measure the vertical polarization, the connections of port 2 and port 3 of the OMT will be exchanged. In Figure 4.2 you can see a photograph of the measurement of port 3.

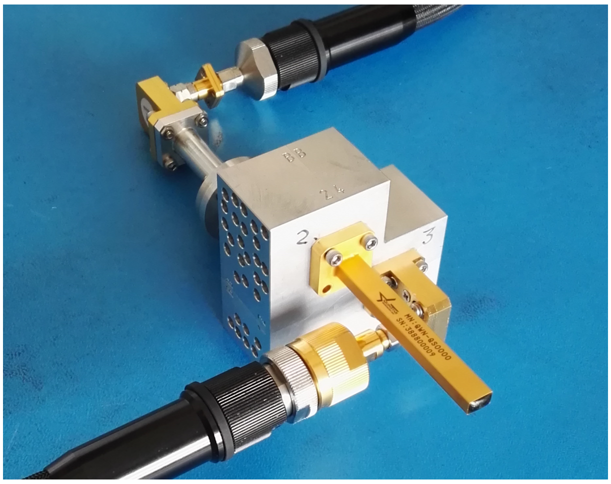

Figure 4.2: Real Insertion Loss Measurements of the OMT Indiviudally

4.1.2 Isolation

For the measurement of the isolation we will use the same scheme of the Figure 4.1. In this case, you must rotate the common port transition by 90° as shown in Figure 4.3, where port 1 of the PNA is rotated 90° with respect to port 2 of the PNA.

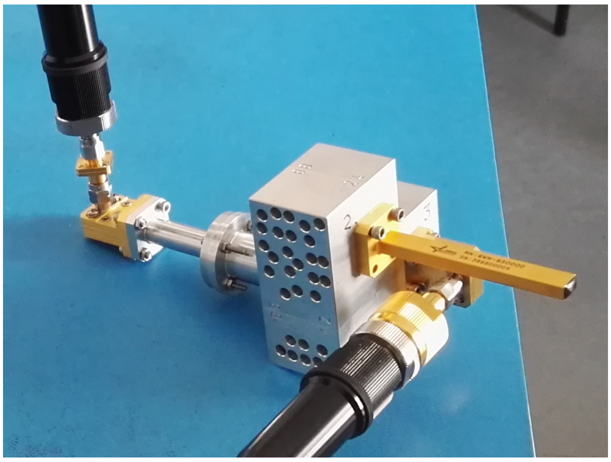

Figure 4.3: Real Isolation Measurements of the OMT Indiviudally

4.1.3 Cross talk

Cross-talk is the transmission of power between rectangular ports. For this measure, OMT must be connected to PNA as indicated in Figure 4.4.

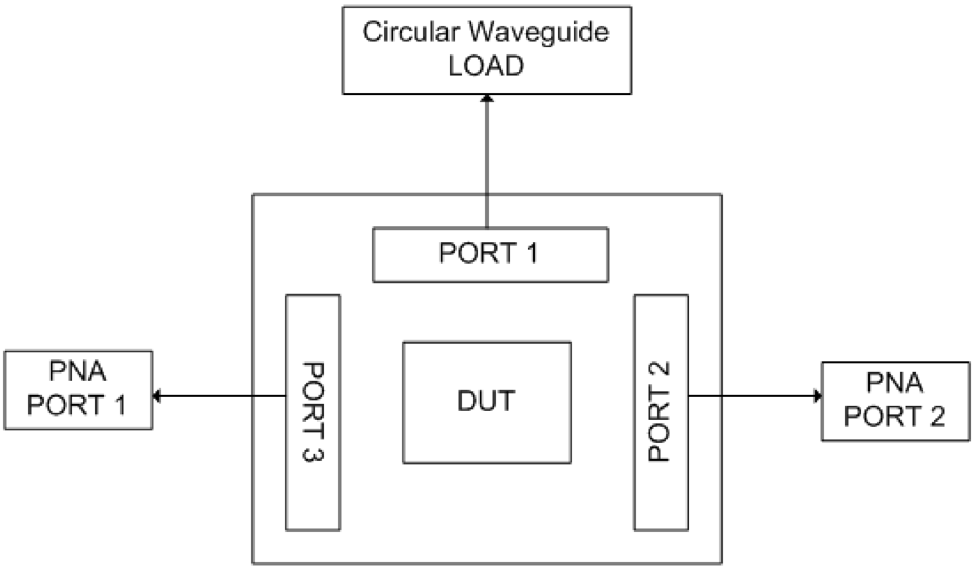

Figure 4.4: Schematic of Cross Talk Measurements of the OMT Indiviudally

The circular port was connected to a rectangular waveguide load (**Appendice F.3**). Rectangular ports of the OMT was connected to the coax-to-waveguide adapters.

Measurement can be seen in Figure 4.5.

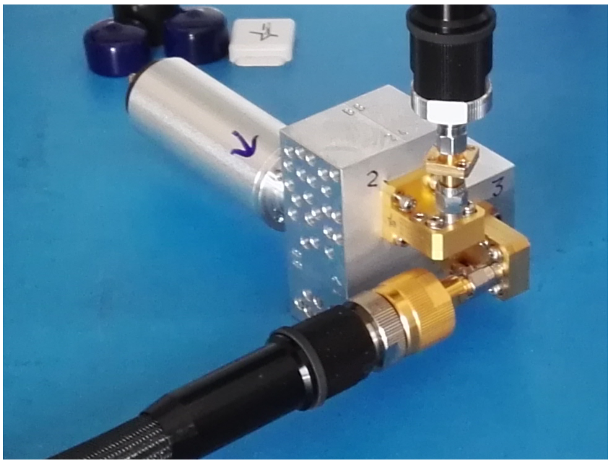

Figure 4.5: Cross-Talk Measurements

4.1.4 Insertion Losses Back-to-Back

To measure insertion losses a Back-to-Back measurement can be made, thus reducing the error introduced by the circular to rectangular guide transition. For this measure the OMT must be connected to the PNA as indicated in Figure 4.6.

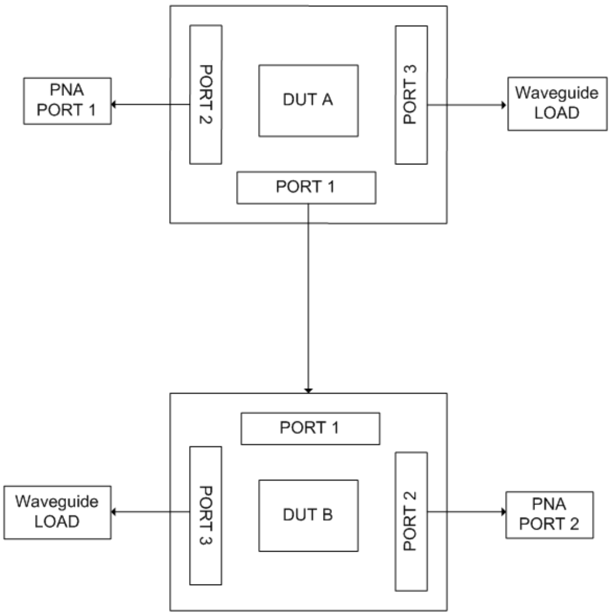

Figure 4.6: Schematic of Insertion Losses Measurements of the Back-to-Back

The circular port of the OMT A was connected to the circular port of the OMT B. The rectangular port of the OMT connected to the analyzer was connected to the coax-to-waveguide adapters. The rectangular port of the OMT not connected to the analyzer was terminated with a rectangular waveguide load.

To measure the insertion losses of the horizontal component the ports will be connected as in Figure 4.6, to measure the losses in the vertical component will be exchanged connections, in port 3 of the OMT will put the port of the PNA And in port 2 of the OMT the load will be connected. Measurement can be seen in Figure 4.7. The results of the measures of OMT A and B will be presented below.

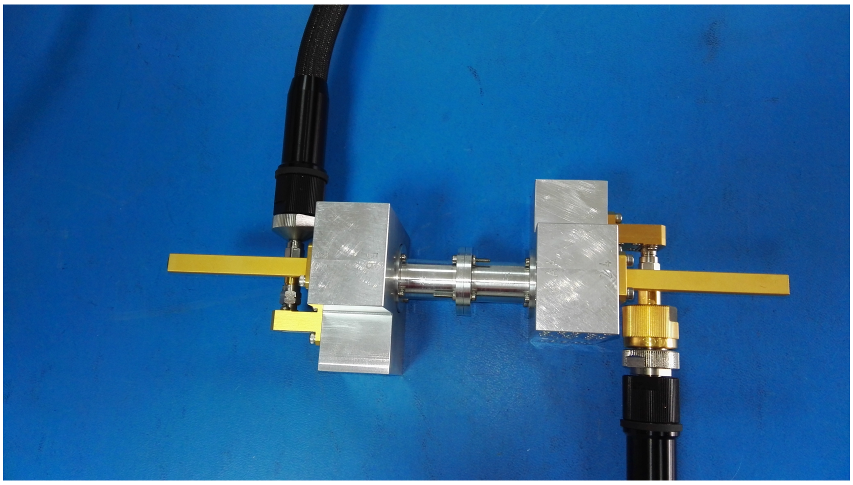

Figure 4.7: Real Back-to-Back Measurement

4.2 OMT A Measurements

The results for OMT A will be shown below. The results obtained for vertical polarization (Port 3) are in Figure 4.8 and data are collected in Table 4.1. Reflections corresponding to the measurement of insertion losses (4.1.1) (since it is possible to measure them in each of the measures defined in 4.1). Insertion losses have been measured by 4.1.1 and isolation by 4.1.2.

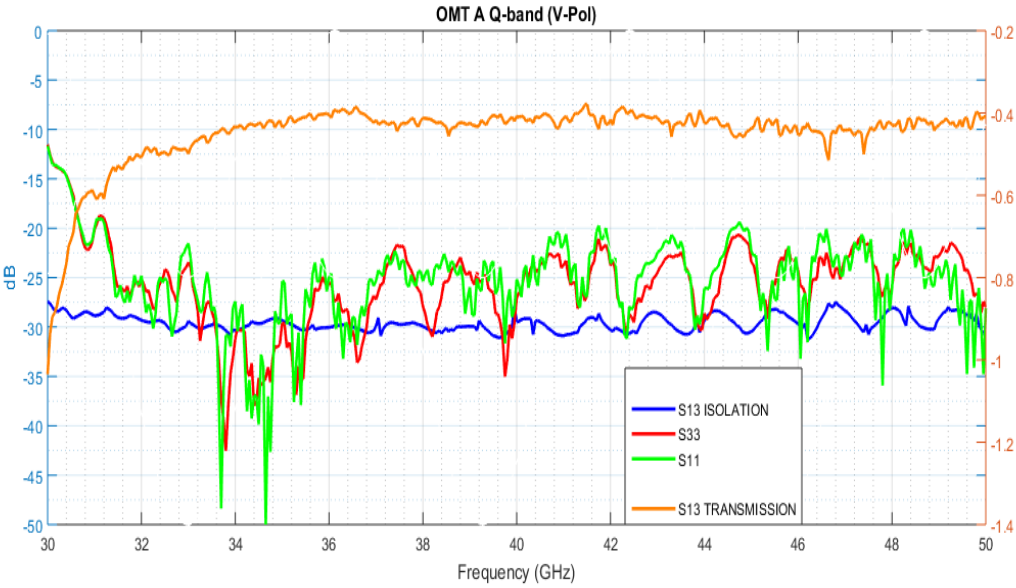

Figure 4.8: OMT A Vertical Polarization S-Parameters

Table 4.1: OMT A Results Vertical Polarization

Parameter	Definition	Value (dB)
S1(1)1(1) & S1(2)1(2) **S33**	Return Loss	>20 >20
S1(1)3	Insertion Loss	<0.6
S1(2)3	Isolation	>25

We think the resonances seen are reflections caused by misalignment of the waveguides used in the measurement.

Results obtained for the horizontal polarization are in Figure 4.9 and data are collected in the Table 4.2.

Results obtained in the Cross-Talk measure (explained in 4.1.4) are in Figure 4.10.

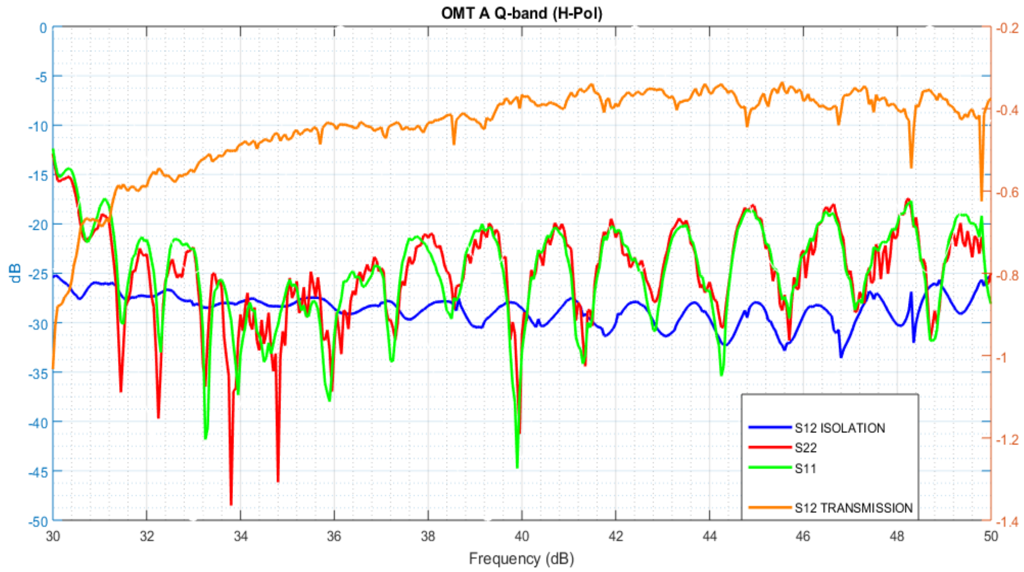

Figure 4.9: OMT A Horizontal Polarization S-Parameters

Table 4.2: OMT A Results Horizontal Polarization

Parameter	Definition	Value (dB)
S1(1)1(1) & S1(2)1(2) **S22**	Return Loss	>18 >20
S1(1)2	Insertion Loss	<0.7
S1(2)3	Isolation	>25

Figure 4.10: OMT A Cross-Talk S-Parameters

It is checked how the return losses are similar to the other two measures. In this case they will be closer to reality because of the waveguide circular load. And cross-talk is less than -40 dB.

4.3 OMT B

Results obtained for the vertical polarization (Port 3) are in Figure 4.11 and the data are collected in the Table 4.3. Reflections correspond to the measurement of insertion losses (measure explained in 4.1.1).

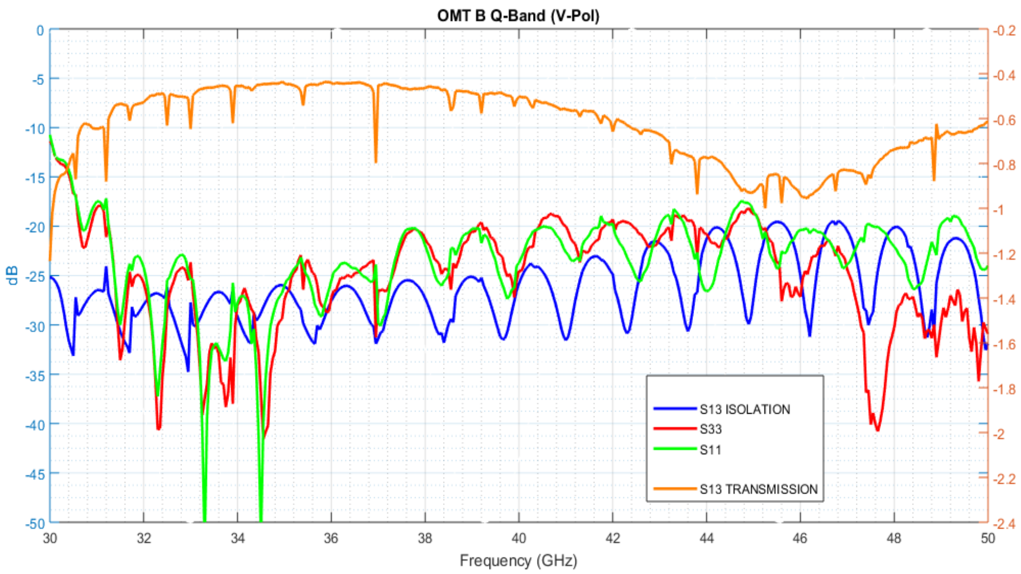

Figure 4.11: OMT B Vertical Polarization S-Parameters

Table 4.3: OMT B Results Vertical Polarization

Parameter	Definition	Value (dB)
S1(1)1(1) & S1(2)1(2) **S33**	Return Loss	>18 >20
S1(1)3	Insertion Loss	<0.8
S1(2)3	Isolation	>20

Results obtained are those of Figure 4.12 and the data are collected in Table 4.4.

Results obtained in the measure of Cross-Talk with the measurement explained in 4.1.3 are in Figure 4.13.

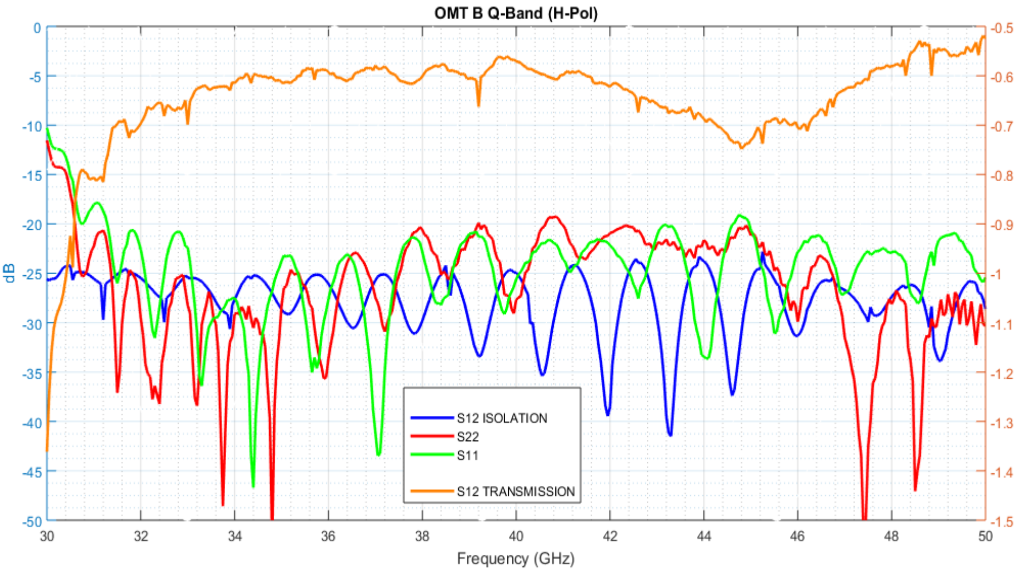

Figure 4.12: OMT B Horizontal Polarization S-Parameters

Table 4.4: OMT B Results Horizontal Polarization

Parameter	Definition	Value (dB)
S1(1)1(1) & S1(2)1(2) **S22**	Return Loss	>18 >20
S1(1)2	Insertion Loss	<0.8
S1(2)3	Isolation	>20

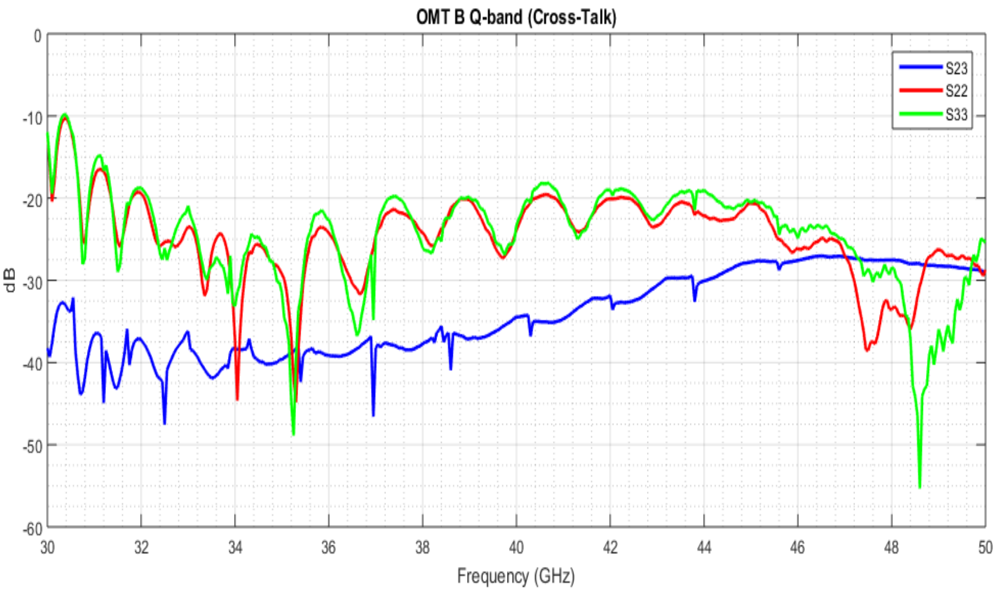

Figure 4.13: OMT B Cross-Talk S-Parameters

It is checked how return losses are similar to the other two measures. In this case they will be closer to reality because of the circular waveguide load. And cross-talk is less than -25 dB.

4.4 Two OMT Measurements

Back-to-back has been performed to measure insertion losses with the measure explained in 4.1.4. Results obtained in B2B for both ports are in Figure 4.14, where transmission losses have been divided by two.

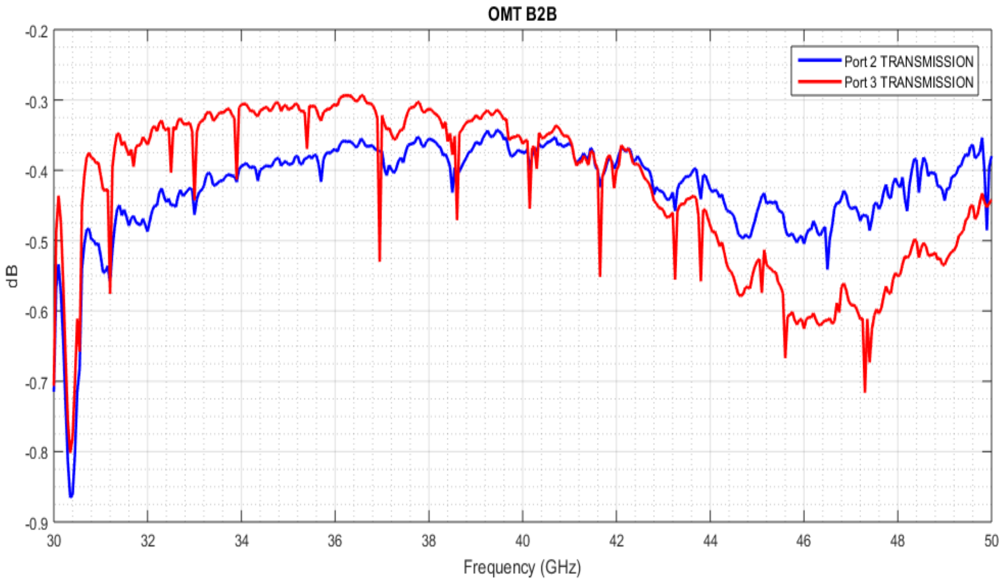

Figure 4.14: B2B Port 3 S-Parameters

It is observed in transmission losses as the envelope is the same as the one of the OMT B that at high frequencies gets worse, but with a smaller value of losses possibly due to the OMT A.

Finally two graphs of intercomparison of the isolation of the two OMTs have been made (Figure 4.15).

From measurement of both OMT it can be shown that OMT A has better characteristics than OMT B, possibly due to machining errors. Both OMT do not fulfill the characteristics of the simulations so we can think that both can also have some Machining error and asymmetry.

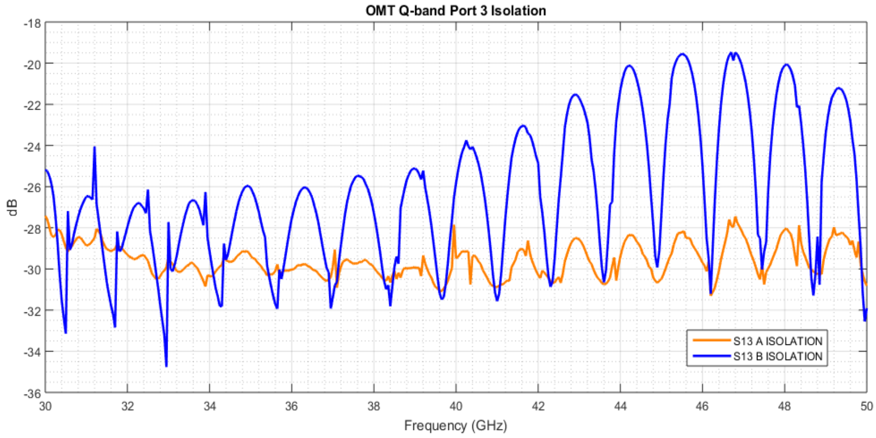

(a) ***Port 3 Isolation***

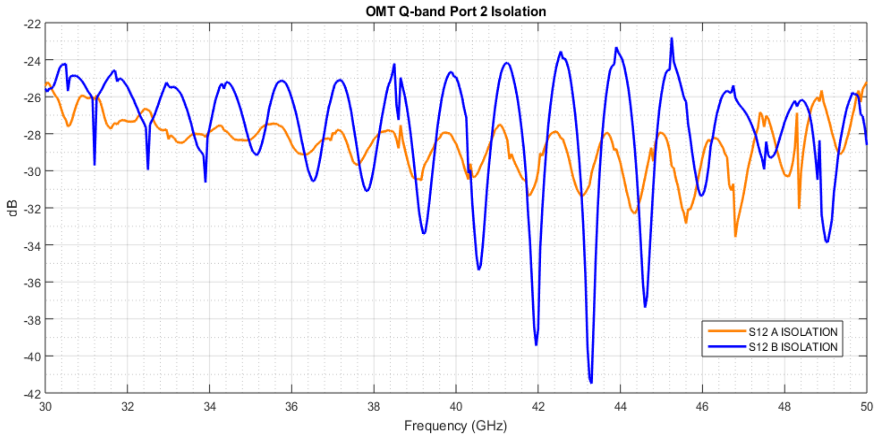

(b) ***Port 2 Isolation***

Figure 4.15: Intercomparison Isolation